Research Article

Journal of Labelled Compounds and Radiopharmaceuticals

Received 13 October 2013, Revised 10 December 2013, Accepted 12 December 2013 Published online 23 January 2014 in Wiley Online Library

(wileyonlinelibrary.com) DOI: 10.1002/jlcr.3183

[18F]Fluoropyruvate: radiosynthesis and initial biological evaluation

Keith Graham,[a]* Andre Müller,[a,b] Lutz Lehmann,[a] Norman Koglin,[a,b] Ludger Dinkelborg,[a,b] and Holger Siebeneicher[a]

The radiosynthesis of [18F]fluoropyruvate was investigated using numerous precursors were synthesized from ethyl 2, 2-diethoxy-3-hydroxypropanoate (5) containing different leaving groups: mesylate, tosylate, triflate, and nonaflate. These precursors were evaluated for [18F]fluoride incorporation with triflate being superior. The subsequent hydrolysis step was investigated, and an acidic hydrolysis was optimized. After establishing suitable purification and formulation methods, the [18F]fluoropyruvate could be isolated in ca. 50% d.c. yield. The [18F]fluoropyruvate was evaluated *in vitro* for its uptake into tumor cells using adenocarcinomic human alveolar basal epithelial cells (A549) and unfortunately showed an uptake of approximately 0.1% of the applied dose per 100,000 cells after 30 min. Initial pharmacokinetic properties were assessed *in vivo* using nude mice showed a high degree of bone uptake from defluorination, which will limit its potential as an imaging agent for metabolic processes.

Keywords: fluorine-18 radiolabeling; PET imaging; fluoropyruvate; pyruvate kinase; pyruvate dehydrogenase

Introduction

Pyruvic acid plays a pivotal role in numerous biochemical pathways, both in the mammalian and bacterial systems. Pyruvate is a substrate for a number of key enzyme systems and different transport mechanisms including the Krebs cycle, monocarboxylic acid transporter (MCT), pyruvate dehydrogenase, lactate dehydrogenase (LDH), and pyruvate kinase.[1] Pyruvate plays a major role in the metabolism of the heart and in addition is believed to play also a key role in cancer cell metabolism as it is one of the metabolism products derived from the cancer cells' enhanced glycolytic activity (also known as the 'Warbung Effect').[2–4] The pyruvate produced during glycolysis acts as a key intermediate between the glycolysis and the Krebs cycle (Figure 1). Part of it can be transported from the cell cytoplasm into the mitochondrial matrix, where it is converted to acetyl coenzyme A which then enters the Krebs cycle. However, in cancer tissues, the majority of pyruvate remains in the cytosol and gets rapidly reduced to lactate by LDH. Lactate is released from the tumor cells by monocarboxylate transporters (MCT4). The reduction step regenerates NAD+ from NADH in the cytosol which is highly needed for a continued conversion of glucose in the glycolysis. Release of lactate from the cells is accompanied with protons, which cause acidification of the tumor microenvironment a process promoting local tumor growth and invasion. Initially, the release of large amounts of lactate was considered as carbon waste, and lactate production is solely needed for the regeneration of NAD. However, more recent studies showed that the released lactate can be taken up and consumed by adjacent tumor cells via MCT1.[5] Another portion of the released lactate enters the blood stream and can be used in the liver to resynthesize glucose in an adopted Cori cycle. A high production rate of lactate can cause lactic acidosis, which is a prominent feature of the tumor microenvironment.[6,7]

Lactate and pyruvate are both described as transporter substrates for MCT1 and MCT4. For MCT1, K_m values of 0.7 and 3–5 mM were described for pyruvate and lactate, respectively. For MCT4, K_m values for L-lactate and pyruvate are 28 and 150 mM, respectively.[8]

A halogenated pyruvate derivative (3-bromopyruvate) is described in literature as potent agent for tumor therapy by inhibiting the glycolytic enzyme hexokinase and causing ATP depleting.[9] It is hypothesized that 3-bromopyruvate enters the tumor cells via MCT4 that release lactate.[9,10] In addition, to support the hypothesis of using pyruvate to image tumors, hyperpolarized [13C]-pyruvate has been recently described for tumor imaging in tumor-bearing rodents and is currently studied in cancer patients.[11] After injection, its conversion to either lactate in tumors or alanine in healthy tissues can be monitored by magnetic resonance spectroscopy.

The only radiolabeled derivatives of pyruvic acid are either [11C]-labeled or [14C]-labeled, of which only the [11C]-derivative would be suitable for non-invasive imaging (Figure 2). The synthesis of [11C]pyruvic acid has been reported either using enzymatic methods[12] or chemical methods.[13,14] This radiopharmaceutical was investigated in tumor-bearing rabbits and enabled clear visualization of the tumor and progressed to clinical trials for brain tumors.[15] These interesting results lead us to investigate whether a [18F]-radiolabeled pyruvate derivative would be a suitable tool for

[a]*Bayer Healthcare, Global Drug Discovery, Müllerstrasse 178, 13353 Berlin, Germany*

[b]*Piramal Imaging, Tegeler Strasse 6-7, 13353 Berlin, Germany*

**Correspondence to: Keith Graham, Bayer Healthcare, Global Drug Discovery, Müllerstrasse 178, 13353 Berlin, Germany.*
E-mail: keith.graham@bayer.com

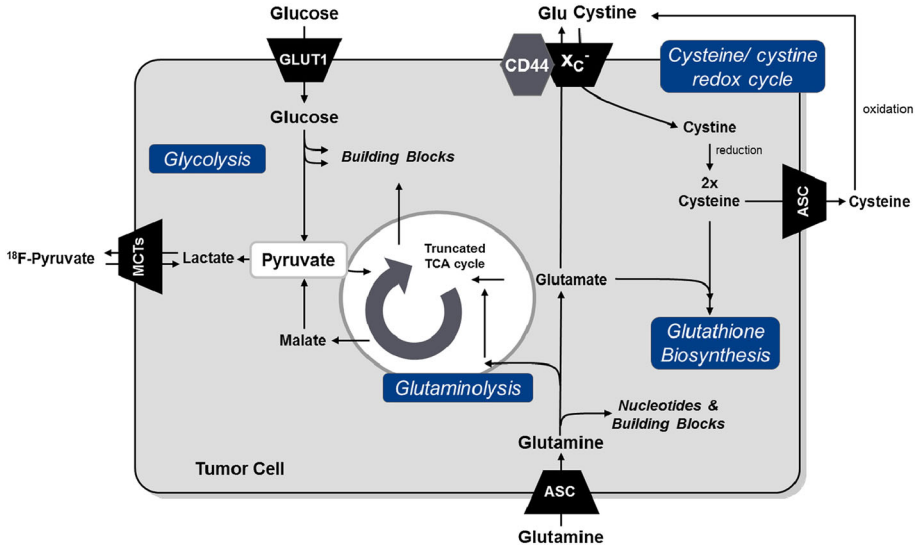

Figure 1. Tumor-specific adaptations of the intermediary metabolism for assuring energy production, growth, ROS protection, and survival. Tumors are characterized by adaptation of several catabolic and anabolic pathways as well as transport systems to meet their demands for energy, growth, and detoxification. In particular, glycolytic and glutaminolytic pathways along with a truncated tricarboxylic acid cycle are pronounced. Pyruvate is a key metabolic intermediate and central hub in intermediary tumor metabolism. [^{18}F]-labeled pyruvate derivatives are supposed to feed into this system via uptake through monocarboxylate transporters. This figure is available in color online at wileyonlinelibrary.com/journal/jlcr

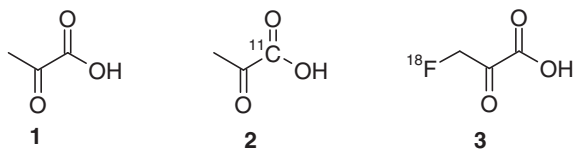

Figure 2. Structures of pyruvic acid (**1**), [^{11}C]labeled pyruvic acid (**2**), and [^{18}F] fluoropyruvate (**3**).

imaging metabolism *in vivo* (Figure 2). Surprisingly, despite fluoropyruvate being commercially available, we could not find a radiosynthesis for [^{18}F]fluoropyruvate described in the literature; the only reference to this tracer was found in a patent application without any experimental details to its synthesis.[16]

Herein, we report on the synthesis of various precursors and their ability to incorporate [^{18}F]fluoride using non-carrier added (n.c.a.) nucleophilic fluorination methods. The subsequent deprotection of the radiolabeled intermediate was evaluated to allow the radiofluorinated derivative [^{18}F]-**3** to be synthesized in good yield and high radiochemical purity. This tracer was evaluated *in vitro* with A549 tumor cells and *in vivo* in nude mice.

Materials and methods

General

Chemicals and solvents were used as received from commercial vendors, Sigma Aldrich (Taufkirchen, Germany), Acros Organics (part of Thermo Fisher-Scientific, Nidderau, Germany). [^{18}F] Fluoride was produced via an ^{18}O(p,n)^{18}F nuclear reaction and was supplied by EuroPET (Berlin, Germany). Chemical reactions were monitored by thin layer chromatography (TLC) and by UPLC/MS analysis of reaction mixtures (Waters Aqcuity with single-quadrupole ESI-MS detector). Crude products were, unless stated otherwise, purified on silica gel (KP-SIL cartridges, Biotage) on automated flash chromatography devices (SP-4 or Isolera Four by Biotage). Nuclear magnetic resonance (NMR) spectra were recorded on ^{1}H, and ^{19}F-NMR spectra were recorded with the Bruker AVANCE-300 and 400 MHz and the Bruker DRX-600 NMR spectrometer. Chemical shifts (δ) are expressed in parts per million relative to tetramethylsilane. Coupling constants (J) are expressed in Hertz (Hz), and the following abbreviations are used to describe the appearance of peak patterns: s (singlet), d (doublet), t (triplet), q (quartet), quint (quintet), and combinations thereof (e.g. dd, doublet of doublet); furthermore, m (multiplet), mc (centered multiplet), and br (broad signal). Purity of all compounds was judged to be in the 95% range according to ^{1}H-NMR, with no chemical impurity detectable. Radioanalytical HPLC runs were performed on an Agilent 1100, and preparative HPLC runs were performed on a Knauer Smartline 1000, both fitted with a GABI Star radioactivity detector (Raytest). Analytical HPLC to check the radiochemical purity and co-injections was performed using a Synergy Hydro RP column (250 × 4.6 mm, 4 μ, Agilent): solvent A, water + 0.1% TFA (v/v); solvent B, acetonitrile + 0.1% trifluoroacetic acid (v/v); gradient, isocratic 0% B for 2 min then 0% B to 30% B in 10 min; flow, 1 mL/min. Semi-preparative HPLC purifications were performed using an ACE RP C18 column (10 × 250 mm; 5 μm; Advanced Chromatographic Technologie): solvent A, water; solvent B, acetonitrile; gradient, isocratic 5% B for 3 min then 5% B to 100% B in 20 min; flow, 3 mL/min.

The tumor cell lines were obtained from ATTC (USA) and maintained according to protocols provided by the supplier. All chemicals used for biological studies were obtained from Sigma Aldrich (Taufkirchen, Germany).

Synthesis of the precursors 6-9

*Ethyl 2,2-diethoxy-3-hydroxypropanoate (**5**)*

n-Butyllithium (4.00 mL, 10 mmol, 2.5 M in hexanes) was added to a solution of diisopropylamine (1.68 mL, 12 mmol) in dry THF (30 mL) under nitrogen at −78°C. After 30 min at 0°C, the mixture was cooled to −78°C, and methyl dimethoxyacetate **4** (1.78 mL, 10 mmol) was added slowly. After 50 min at −78°C, paraformaldehyde

(1.2 g, 40 mmol) was added and allowed to warm to RT. After 2 h at RT, saturated $NaHCO_{3(aq)}$ was added. The reaction was diluted with water extracted with EtOAc. The organic layers were dried (MgSO4) and filtrated. After evaporation, the crude mixture was purified via flash chromatography with hexane/EtOAc (6:1) to give **5** as a colorless oil (835 mg, 40%). ^{1}H-NMR (400 MHz, $CDCl_3$): $\delta = 1.26$ (t, $J = 7.06$ Hz, 6H) 1.33 (t, $J = 7.06$ Hz, 3H) 1.92 (br s, 1H) 3.51–3.73 (m, 4H) 3.82 (br s, 2H) 4.29 (q, $J = 7.16$ Hz, 2H) ppm. ^{13}C-NMR (100 MHz, $CDCl_3$): $\delta = 14.19$, 15.24, 58.40, 61.81, 63.23, 100.57, 168.65 ppm.

*Ethyl 2,2-diethoxy-3-[(methylsulfonyl)oxy]propanoate (**6**)*

5 (206 mg, 1.00 mmol) and triethylamine (205 μL, 1.49 mmol) were dissolved in CH_2Cl_2 (7 mL) and cooled to 0°C. A solution of methanesulfonyl chloride (77 μL, 0.99 mmol) in CH_2Cl_2 (3 mL) was added slowly. The reaction was gradually warmed to room temperature and stirred for additional 5 h. The reaction mixture was diluted with water and extracted with methylene chloride. The organic layers were dried ($MgSO_4$) and filtrated, concentrated and purified by column chromatography (SiO2:hexanes/EtOAc 5:1) to give **6** as a colorless oil (277 mg, 97%). ^{1}H-NMR (400 MHz, $CDCl_3$): $\delta = 1.26$ (t, $J = 7.07$ Hz, 6H), 1.34 (t, $J = 7.20$ Hz, 3H), 3.07 (s, 3H), 3.51–3.59 (m, 2H), 3.63–3.70 (m, 2H), 4.30 (q, $J = 7.16$ Hz, 2H), 4.44 (s, 2H) ppm. ^{13}C-NMR (100 MHz, $CDCl_3$): $\delta = 14.22$, 15.08, 38.16, 58.69, 62.24, 67.17, 98.66, 167.02 ppm. MS (ESI): $[M + Na]^+ = 307$.

*Ethyl 2,2-diethoxy-3-{[(4-methylphenyl)sulfonyl]oxy}propanoate (**7**)*

5 (206 mg, 1.00 mmol) was dissolved in a mixture of CH_2Cl_2 (3 mL), Et_3N (150 μL, 1.08 mmol), and DMAP (25 mg, 0.21 mmol) and cooled to 0°C. A solution of *para*-toluenesulfonyl chloride (191 mg, 1.00 mmol) in CH_2Cl_2 (2 mL) was added dropwise. After stirring at 0°C for 5 h, the mixture was washed with water, saturated $NaCl_{(aq)}$, dried over $MgSO_4$, and filtrated. After evaporation, the crude mixture was purified via flash chromatography with hexane/EtOAc (7:1) to give **7** as a colorless oil (212 mg, 59 %). ^{1}H-NMR (400 MHz, $CDCl_3$): $\delta = 1.17$–1.27 (m, 9H), 2.45 (s, 3H), 3.40–3.59 (m, 4H), 4.18 (q, $J = 7.16$ Hz, 2H), 4.21 (s, 2H), 7.35 (d, $J = 8.10$ Hz, 2H), 7.78 (d, $J = 8.48$ Hz, 2H) ppm. ^{13}C-NMR (100 MHz, $CDCl_3$): $\delta = 14.11$, 15.03, 21.71, 58.42, 62.08, 67.09, 98.33, 128.14, 129.85, 132.47, 145.10, 166.76 ppm. MS (ESI): $[M + Na]^+ = 383$.

*Ethyl 2,2-diethoxy-3-{[(trifluoromethyl)sulfonyl]oxy}propanoate (**8**)*

To a solution of **5** (309 mg, 1.5 mmol) in dry CH_2Cl_2 (10 mL) was added pyridine (157 μL, 1.95 mmol). After cooling to −78°C, trifluoromethylsulfonyl anhydride (328 μL, 1.95 mmol) was added dropwise. The mixture was stirred at 0°C for 1 h. The reaction was quenched with saturated $NH_4Cl_{(aq)}$ and extracted with CH_2Cl_2 three times. The combined organic layers were dried over Na_2SO_4 and concentrated. The crude residue was purified by silica gel flash chromatography with EtOAc/hexane (1:10) to give **8** as a colorless oil (430 mg, 85%). ^{1}H-NMR (400 MHz, $CDCl_3$): $\delta = 1.22$–1.30 (m, 6H) 1.34 (t, $J = 7.16$ Hz, 3H) 3.49–3.75 (m, 4H) 4.32 (q, $J = 7.16$ Hz, 2H) 4.64 (s, 2H) ppm. ^{19}F-NMR (376 MHz, $CDCl_3$): $\delta = -74.32$ ppm.

*Ethyl 2,2-diethoxy-3-{[(nonafluorobutyl)sulfonyl]oxy}propanoate (**9**)*

To a stirred solution of **5** (172 mg, 0.83 mmol) in MeCN (7.0 mL) was added perfluoro-1-butanesulfonyl fluoride (180 μL, 1.00 mmol), *i*-$Pr_2NEt(HF)_3$ (270 μL, 1.08 mmol), and *i*-Pr_2NEt (543 μL, 3.17 mmol) at 0°C. After stirring at 25°C for 5 h, the mixture was quenched with water, extracted with EtOAc, washed with saturated $NaCl_{(aq)}$, dried over $MgSO_4$, and concentrated. The crude mixture was purified via flash chromatography with hexane/EtOAc (5:1) to give **9** as a colorless oil (194 mg, 0.4 mmol, 48%). ^{1}H-NMR (400 MHz, $CDCl_3$): $\delta = 1.26$ (t, $J = 7.06$ Hz, 6H) 1.34 (t, $J = 7.16$ Hz, 3H) 3.50–3.73 (m, 4H) 4.31 (q, $J = 7.03$ Hz, 2H) 4.68 (s, 2H) ppm. ^{19}F-NMR (376 MHz, $CDCl_3$) $\delta = -126.09$ to −125.67 (m, 2F) −121.51 to −121.14 (m, 2F) −110.76 to −110.39 (m, 2F) −80.64 (t, $J = 9.75$ Hz, 3F) ppm. ^{13}C-NMR (100 MHz, $CDCl_3$): $\delta = 14.04$, 15.00, 58.91, 62.49, 72.52, 97.76, 166.11 ppm. MS (ESI).

*Radiosynthesis of [^{18}F]fluoropyruvate (**3**)*

[^{18}F]Fluoride was produced by an ^{18}O (p, n) ^{18}F nuclear reaction by bombardment of a 98% ^{18}O-enriched water target with an 11 MeV proton beam at the RDS111 cyclotron. The aqueous [^{18}F]fluoride solution was trapped in a small anion exchange Sep-PakTM Plus QMA cartridge (Waters) (preconditioned with 5 mL 0.5 M K_2CO_3 solution and 10 mL water). The radioactivity was eluted with a solution mixture (1.0 mg K_2CO_3 in 0.5 mL water and 5.27 mg K_{222} in 1.5 mL MeCN) from the QMA cartridge into a 5 mL conic Wheaton vial. The solvent was evaporated under a stream of nitrogen at 110°C. Azeotropic drying was repeated three times with 1.0 mL portions of acetonitrile. Then, the precursor ethyl 2,2-diethoxy-3-{[(trifluoromethyl)sulfonyl]oxy} propanoate (**8**) (4.5 mg, 13.3 μmol) in dry MeCN (300 μL) was added to the dried [^{18}F]KF–K_{222}. After heating at 90°C for 15 min in a sealed vial, the reaction mixture was diluted with 1.7 mL water and given on a semi-prep HPLC (ACE, RP C18, (10 × 250 mm), 5 μ, 3 mL/min (Agilent), solvent A: H_2O, solvent B: MeCN, gradient: isocratic 5% B for 3 min then 5% B to 100% B in 20 min, retention time of ethyl 2,2-diethoxy-3-[^{18}F] fluoropropanoate: 20.9–21.1 min). The collected fraction (1.0–1.2 mL) was given into a 5 mL conic Wheaton vial, and 4 N H_2SO_4 (600 μL) was added. The vial was sealed and the reaction mixture heated for 20 min at 140°C. Afterwards, the reaction mixture was neutralized with 6 N NaOH, and under gentle stream of nitrogen, the reaction mixture was heated in the open Wheaton vial at 100°C to dryness (20–30 min). The residue was taken up in Ampuwa® water (5000 μL) to get 23–325 MBq [^{18}F] fluoropyruvate (radiochemical yield, 25 ± 11.4% d.c; synthesis time, 145 ± 13.4 min; n = 4). The radiochemical purity was >95%. The [^{18}F]-labeled product was confirmed by co-injection with the F-19 cold standard on an analytical HPLC (column: Synergy Hydro RP, 250 × 4.6 mm, 4 μ, 1 mL/min (Agilent); solvent A, H_2O + 0.1% TFA; solvent B, MeCN + 0.1% TFA; gradient, isocratic 0% B for 2 min then 0% B to 30% B in 10 min). This co-injection was also spiked with [^{18}F]fluoride, and the baseline separation of the [^{18}F]fluoride peak from the product peak showed a resolvable product retardation from the void on the used Synergy Hydro column. In addition, silica TLC, using the solvent system 1-butanol:water:acetic acid:ethanol (12:5:3:3), was carried out with the [^{18}F]-labeled product, fluoropyruvate, and [^{18}F]-fluoride; the fluoride remained on the baseline, and both the radiolabeled [18F]fluoropyruvate and fluoropyruvate gave the same R_f value of 0.49.

Cell lines

For tracer uptake and competition studies A549 tumor cells were used. Twenty-five thousand cells/well were seeded in 48 well plates 2 days prior to the cell uptake study and grown under standard conditions (37°C, 5% CO_2) until sub-confluency. The cell number at the day of the uptake assay was determined by detaching cells in three representative wells and cell counting

in a Neubauer cell chamber. Uptake data were normalized to 100,000 cells. Prior to the radioactive uptake assay, the cell culture medium was removed, and the cells were washed twice with 37°C warm PBS buffer. The radiotracer was added to the assay buffer (PBS/0.1% w/v BSA) using a concentration of 250 kBq/well. For competition experiments, the cells were co-incubated with pyruvate as competitor used in excess of 1 mM. Tracer uptake was stopped by removal of the assay buffer at the time points indicated. Cells were quickly washed twice with PBS and lysed by the addition of 1 N NaOH. The cell lysate was removed from the plates, and radioactivity of ^{18}F-samples was determined in a gamma counter (Wizard 3, Perkin Elmer, USA).

Animals

The animal positron emission tomography (PET) imaging study was performed in compliance with the current version of the German law concerning animal protection and welfare. NMRI nude mice (Taconic, Ry, Denmark) were used for this study. A PET imaging study was performed using the Inveon small animal PET/computed tomography (CT) scanner (Siemens, Knoxville, TN). Ten megabecquerel of ^{18}F-fluoropyruvate was injected intravenously in conscious animals via the tail vain. After 50 min post-injection (p.i.), the animals were anesthetized with isoflurane (Abbot), and the PET data were acquired from 60 to 70 min p.i.

Results

Synthesis of the precursors 6-9

As outlined in Scheme 1, the key alcohol intermediate **5** was synthesized in moderate yield via deprotonation of dimethoxy acetate **4** with lithium diisopropylamide generated *in situ* and subsequent use of paraformaldehyde as the elecrophile. This key intermediate was reacted with methanesulfonyl chloride, para-toluenesulfonyl chloride, trifluoromethylsulfonyl anhydride, or perfluoro-1-butanesulfonyl fluoride using standard chemistry to yield the mesylate (**6**), tosylate (**7**), triflate (**8**), or nonafluoro butylsulfonate (**9**), respectively.

Radiolabeling of the precursors 6-9

To establish a suitable radiosynthesis method of [^{18}F]fluoropyruvate, the n.c.a. nucleophilic [^{18}F]fluorination was evaluated using the mesylate (**6**), tosylate (**7**), triflate (**8**), and nonafluorobutylsulfonate (**9**) precursors. Numerous conditions were tested with the four precursors, that is, different solvents (MeCN, DMSO, and DMF), different temperatures (90–160°C), and different times (5–20 min) are illustrated in Table 1, where it is clear to see that the triflate precursor **8** was superior with excellent incorporation under relatively mild conditions. The radiolabeled intermediate **5** was purified by semi-preparative HPLC methods before the hydrolysis step as we believed this would simplify the process as a purification after the hydrolysis step could prove to be non-trivial as the polar [^{18}F]fluoropyruvate would have to be separated from other polar impurities, both radioactive and non-radioactive (Scheme 2).

Deprotection of the radiolabeled intermediate 10

The hydrolysis of the purified [^{18}F]-labeled intermediate [^{18}F]-**5** was tested under both acidic and basic conditions. Basic hydrolysis was tested with 2 M NaOH at 25°C and was complete after 10 min with no defluorination observed; a second acidic step was tested under 6 M HCl at 120°C for 15 min. To simplify the synthesis, the acidic conditions were tested as this would enable a one-step deprotection. Therefore, the intermediate [^{18}F]-**5** was subjected to different strongly acidic deprotection conditions (2–6 M HCl and 2–4 M H_2SO_4) using varied temperatures and times, and the results are summarized in Table 2. The hydrolysis conditions were monitored by HPLC and TLC (*n*-BuOH:water:AcOH:EtOH, 12:5:3:3), and 4 M H_2SO_4 at 100°C for 20 min were found to be the optimal conditions. The resulting strongly acidic reaction mixture was neutralized, evaporated to dryness, and taken up in 5 mL Ampuwa® water to give the desired product [^{18}F]fluoropyruvate **3** as a formulated solution ready for biological testing. The identity of [^{18}F]fluoropyruvate **3** was confirmed by co-injection of the corresponding cold reference fluoropyruvate (Figure 3A and B) and also injected with free [^{18}F]fluoride (Figure 3C) to confirm that the polar product peak was not free [^{18}F]fluoride.

Biological characterization

The uptake of ^{18}F-fluoropyruvate was studied in A549 tumor cells. After 10 min of incubation, a tracer uptake/binding of 1752 ± 504 cpm per 100,000 cells was measured, which corresponds to 0.08% of the applied dose. In a 10 min blocking experiment using excess of pyruvate (1 mM), the uptake was slightly reduced to 1216 ± 107 cpm per 100,000 cells corresponding to 0.05% of the applied dose. No increasing tracer uptake was observed for the following time points. The 20 min uptake value

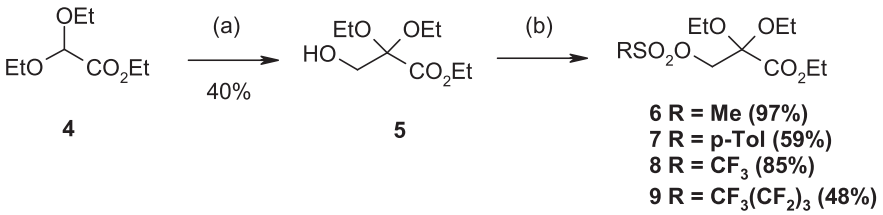

a) i) LDA, THF, -78°C to 0°C; ii) paraformaldehyde, 0°C (40%);
b) R = Me: MsCl, Et_3N, DCM, RT;
R = p-Tol: TsCl,DMAP, Et_3N, DCM, RT;
R = CF_3: Tf_2O, pyridine, DCM, -78°C to 0°C;
R = $CF_3(CF_2)_3$: $C_4F_9SO_2F$, $iPr_2NEt.3HF$, iPr_2NEt, MeCN, RT

Scheme 1. Synthesis of radiolabeling precursors **6-9**.

Table 1. Evaluation of the precursors **6-9** under different radiolabeling conditions

Precursor	Solvent	Temperature (°C)	Time (min)	Incorporation (%)
Mesylate **6**	MeCN	90	10	0
	DMF	120	10	0
	DMSO	160	10	23
Tosylate **7**	MeCN	90	10	0
	DMF	120	10	0
	DMSO	160	10	11
Triflate **8**	MeCN	90	5	77
	MeCN	90	10	82
	MeCN	90	20	97
	DMF	120	10	83
	DMSO	160	10	49
Nonaflate **9**	DMF	120	10	81

Standard conditions of 5 mg K_{222}, 1 mg K_2CO_3, and 4 mg precursor in 300 µL solvent were investigated.

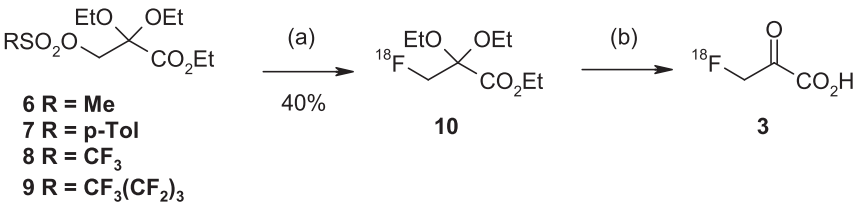

a) K[^{18}F]F, K_{222}, see Table 1 for conditions; b) acidic hydolysis see Table 2 for conditions

Scheme 2. Radiosynthesis of [^{18}F]fluoropyruvate.

Table 2. Evaluation of the hydrolysis of **10** to [^{18}F] fluoropyruvate **3**

Acid	Molarity (M)	Temperature (°C)	Time (min)	Hydrolysis (%)
HCl	2	25	10	0
	2	100	5	15
	6	160	10	23
H_2SO_4	2	140	5	49
	2	160	5	91
	4	140	10	>95
	4	140	20	>95

was higher (3009 ± 2457 cpm per 100,000 cells corresponding to 0.13% of the applied dose) but associated with a higher standard deviation and thus statistically not significant. The 30 min time point was again in the range of 10 min point (1647 ± 421 cpm per 100,000 cells, corresponding to 0.08% of the applied dose) (Figure 4).

Micro-positron emission tomography/computed tomography imaging

A PET/CT imaging study was conducted to study the behavior of the new radiotracer *in vivo*. PET images were acquired at 60 min p.i. Axial, coronal and sagittal sections, and a whole body projection are shown (Figure 5).

Discussion

Our efforts have been focused on investigating and developing new [^{18}F]labeled metabolic tracers that could potentially address the downfalls of [^{18}F]FDG (the PET imaging 'workhorse'), that is, differentiation between tumor and inflammation.[17] These new tracers could offer complimentary imaging tools to answer key clinical questions and help offer patients the best and appropriate treatment. We have reported on a number of glutamate tracers, 4-[^{18}F]fluoroglutamate (BAY 858050)[18] and FSPG (BAY 949392)[19] which were successful in preclinical studies for tumor imaging and showed no uptake in inflammation. Both these tracers progressed to the clinical setting where FSPG proved superior and is being investigated further.[20,21] Multiple mechanisms and many metabolic pathways are adapted in the metabolism of tumor cells. They are connected and converge to support rapid energy generation, to increase biosynthesis of macromolecules, to maintain appropriate cellular redox status, and detoxification potential.[22] These include the aerobic glycolytic, glutaminolytic, and lipogenesis pathway that provide key intermediates for anabolic or anaplerotic reactions.

Pyruvate is a particularly interesting molecule as it is involved in numerous metabolism pathways and, that is, glycolysis, Krebs cycle, MCT, pyruvate dehydrogenase, LDH, and pyruvate kinase.[1] Surprisingly, despite being an attractive molecule for the PET imaging of various disease progresses either in oncology or cardiology, there are very few radiolabeled derivatives of pyruvate and only one PET imaging probe synthesized ([^{11}C] pyruvate) either by enzymatic[12] or chemical methods.[13,14] Interestingly, [^{11}C]pyruvate has been investigated pre-clinically

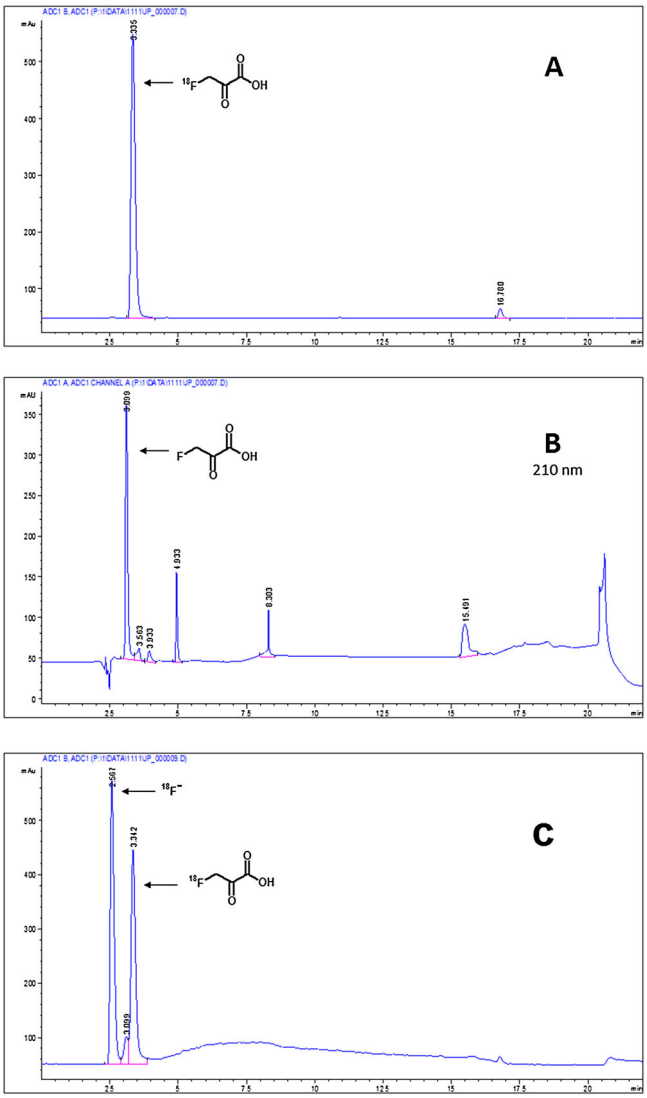

Figure 3. Analytical HPLC chromatograms of the final formulated [^{18}F] fluoropyruvate (**3**) (Figure 3A gamma detector); the co-injection of the [^{18}F] fluoropyruvate (**3**) with fluoropyruvate (Figure 3B, UV detector at 210 nm); and co-injection with [^{18}F]fluoride (Figure 3C gamma detector). This figure is available in color online at wileyonlinelibrary.com/journal/jlcr

in tumor-bearing rabbits, in one patient with a brain tumor[15] which looked promising and in patients with cerebral ischemic hypoxia or infarction.[23] Because of the short half-life of carbon-11, we decided to look into a fluorine-18 derivative as fluoropyruvic acid is a known substrate for pyruvate carboxylase,[24] LDH[25] and inhibitor of the pyruvate dehydrogenase complex,[26,27] and is considerably less toxic than fluoroacetate.[28] Surprisingly, in the literature, the only reference to [^{18}F]fluoropyruvic acid was found in a patent application where no radiosynthesis was described.[16]

In designing a suitable precursor for the synthesis of [^{18}F] fluoropyruvic acid **3**, it seemed that pursing a simple precursor such as simple alkyl esters of bromopyruvic acid, which are commercially available, might not be advantageous as it is known that simple esters of pyruvic acid undergo spontaneous hydration,[29] which we believed would hinder the radiofluorination.

Our strategy was to investigate precursors with the ketone moiety at the two-position protected as a ketal, which should facilitate a quick and simple removal under acidic conditions. The leaving groups for the n.c.a. radiofluorinations would be

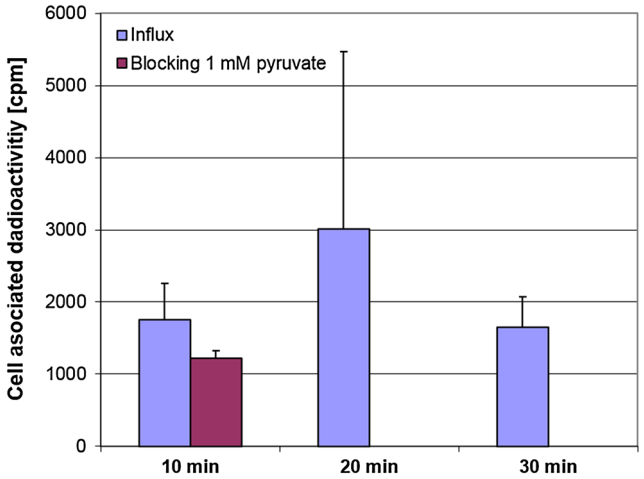

Figure 4. Cell assay to study the uptake of [^{18}F]fluoropyruvate in A549 tumor cells. Cell uptake/binding was measured at 10, 20, and 30 min incubation. A blocking was performed by co-incubation with excess pyruvate (1 mM). Twenty-three thousand counts per minute corresponds to 0.1% of the applied dose. This figure is available in color online at wileyonlinelibrary.com/journal/jlcr

different sulfonates as these are the leaving groups of choice for aliphatic radiofluorinations.[30] In order to synthesize these precursors, the commercially available methyl dimethoxyacetate **4** was treated with lithium diisopropylamide and the electrophile paraformaldehyde to give the key intermediate alcohol, ethyl 2,2-diethoxy-3-hydroxypropanoate **5**, in moderate yield (40%) as illustrated in Scheme 1. Simple standard sulfonation methods on the alcohol **5** gave the desired precursors with the mesylate **6** (97%), tosylate **7** (59%), and triflate **8** (85%) leaving groups. The precursor with the nonaflate **9** leaving group was isolated from unsuccessfully attempts to make the cold fluorine-19 reference compound of **10** using the *Vorbrüggen* fluorination methodology.[31] The radiofluorination was explored using standard radiofluorination methods using Kryptofix 2.2.2 (K_{222}, 5 mg) as the phase transfer catalyst and potassium carbonate (1 mg) as the base. Initial radiolabelings with the standard solvents and temperatures (acetonitrile at 100°C, DMF at 120°C, and DSMO at 160°C) showed that the triflate was the superior precursor with >90% incorporation of fluoride (90°C in acetonitrile for 20 min). The radiolabeled intermediate **10** was purified using semi-preparative HPLC methods as we envisioned difficulties in purifying the final radiolabeling product away from similar polar by-products which could interfere with any subsequent biological testing. The deprotection step on the HPLC purified intermediate **10** was investigated, first under basic condition using 2 M NaOH at RT, and the hydrolysis was found to be quantitative after 10 min with no free [^{18}F]fluoride by TLC analytics. The ketal protecting group was removed by treating basic solution with 6 M HCl and heating at 120°C for 15min which gave the desired [^{18}F]fluoropyruvic acid **3**. The deprotection step was investigated further to see whether a simple acidic deprotection step would be sufficient instead of the two step hydrolysis. The acidic hydrolysis conditions were tested using different molarities (2–6 M) of either HCl or H_2SO_4 at elevated temperatures as shown in Table 2. This single acidic hydrolysis step was not so straightforward as envisioned, and only 4 M H_2SO_4 with heating at 120°C for 10 min or longer was successful. After formulation, the identity of [^{18}F]fluoropyruvic acid **3** was confirmed by co-injection of the corresponding cold reference (Figure 3A and B). [^{18}F]Fluoropyruvic acid **3** was

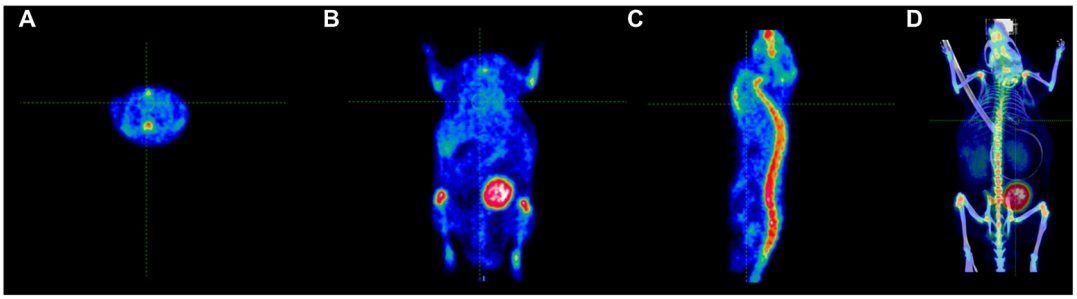

Figure 5. Micro-positron emission tomography/computed tomography (PET/CT) study of [^{18}F]fluoropyruvate in mice. PET data acquisition was started at 60 min after injection of 10 MBq in conscious animals. Corresponding axial (A), coronal (B), and sagittal (C) sections covering the heart and vertebra are shown. Whole body PET/CT is shown in (D). Low PET signals were observed from most tissues except the bone (especially vertebra and joints) and bladder. The increased bone signal is presumably caused by defluorination and the bladder signal from renal excretion. This figure is available in color online at wileyonlinelibrary.com/journal/jlcr

analyzed by HPLC to confirm that no co-elution was observed with free [^{18}F]fluoride (Figure 3C).

By targeting MCTs with [^{18}F]fluoropyruvate, we tried to visualize a common metabolic adaptation in tumor cells. A549 cells are known to have a glycolytic phenotype by consuming glucose and releasing lactate. Therefore, strong MCT activity can be assumed. However, the degree of uptake of [^{18}F] fluoropyruvate in A549 tumor cells was low, and no time dependent uptake was observed, which is in contrast to other ^{18}F-labeled compounds studied in this assay (Figure 4).[18,19] This may suggest that [^{18}F]fluoropyruvate is either not recognized by the transporter or binds with a low affinity that is not sufficient for transport into the cells. This was unexpected in light of the uptake and biological activity of 3-bromopyruvate in cancer cells and the uptake and intracellular conversion of hyperpolarized-[^{13}C]pyruvate. As the fluoropyruvate is known to form mainly the hydrated isoform in aqueous solutions[32] whereas bromopyruvate is mainly present in the ketoform, this slight difference could be a reason for the different uptake behavior of these homologuous compounds.

Positron emission tomography-imaging study in nude mice demonstrated that ^{18}F-fluoropyruvate is quickly excreted via the kidneys into the bladder (Figure 5). Neither the heart nor other organs showed accumulation and retention of the tracer except the bones. The observed uptake of radioactivity can be most likely attributed to accumulation of released free ^{18}F-fluoride after metabolism in the blood and liver as reported for other non-stable ^{18}F-compounds.[18]

More detailed research would be needed to further characterize this new ^{18}F-labeled tracer, however, its low stability in mice limits its use and further exploration *in vivo*.

Conclusions

The synthesis of four precursors (**6-9**) derived from ethyl 2,2-diethoxy-3-hydroxypropanoate **5** bearing the mesylate, tosylate, triflate, and nonaflate leaving groups was successfully synthesized and evaluated for the their ability to incorporate [^{18}F]fluoride. The triflate precursor 8 was found to give the best results. The subsequent hydrolysis step was investigated and optimized to give the desired [^{18}F]fluoropyruvate in an excellent 50% d.c. yield. This tracer was tested *in vitro* resulting in low uptake into adenocarcinomic human alveolar basal epithelial A549 cells. *In vivo* PET imaging of the compound showed considerable defluorination that would limit the use of this tracer as an imaging agent for cancer, although the metabolic degradation pathway in humans might be different than observed in mice.

Acknowledgements

The authors would like to acknowledge the excellent technical assistance of Jörg Pioch, Melanie Senftleben, Jörg Jannsen, and Eva-Maria Bickel.

References

[1] A. L. Lehninger, D. L. Nelson, M. M. Cox, Principles of Biochemistry, 2nd ed. Worth, New York, **1993**.
[2] M. G. Vander Heiden, L. C. Cantley, C. B. Thompson, *Science* **2009**, *324*, 1029.
[3] H. R. Christofk, M. G. Vander Heiden, M. H. Harris, A. Ramanathan, R. E. Gerszten, R. Wie, M. D. Fleming, S. L. Schreiber, L. C. Cantley, *Nature* **2008**, *452*, 230.
[4] M. G. Vander Heiden, J. W. Locasale, K. D. Swanson, H. Sharfi, G. J. Heffron, D. Amador-Noguez, H. R. Christofk, G. Wagner, J. D. Rabinowitz, J. M. Asara, L. C. Cantley, *Science* **2010**, *329*, 1492.
[5] P. Sonveaux, F. Végran, T. Schroeder, M. C. Wergin, J. Verrax, Z. N. Rabbani, C. J. De Saedeleer, K. M. Kennedy, C. Diepart, B. F. Jordan, M. J. Kelley, B. Gallez, M. L. Wahl, O. Feron, M. W. Dewhirst, *J. Clin. Invest.* **2008**, *118*, 3930.
[6] N. C. Denko, *Nature Rev. Cancer* **2008**, *8*, 705.
[7] J. L. Chen, J. E. Lucas, T. Schroeder, S. Mori, J. Wu, J. Nevins, M. Dewhirst, M. West, J.-T. Chi, *PLoS Genet.* **2008**, *4*, e1000293.
[8] A. P. Halestrap, D. Meredith, *Pflugers Arch.* **2004**, *447*, 619.
[9] Y. H. Ko, B. L. Smith, Y. Wang, M.G. Pomper, D. A. Rini, M. S. Torbenson, J. Hullihen, P. L. Pedersen, *Biochem. Biophys. Res. Commun.* **2004**, *324*, 269.
[10] J. P. Geschwind, C. S. Georgiades, Y. H. Ko, P. L. Pedersen, *Expert Rev. Anticancer Ther.* **2004**, *4*, 449.
[11] K. Golman, R. I. Zandt, M. Lerche, R. Pehrson, J. H. Ardenkjaer-Larsen, *Cancer Res.* **2006**, *66*, 10855.
[12] M. B. Cohen, L. Spolter, C. C. Chang, J. S. Cook, N. S. MacDonald, *Int. J. Appl. Radiat. Isot.* **1980**, *31*, 45.
[13] M. R. Kilbourn, M. J. Welch, *Int. J. Appl. Radiat. Isot.* **1982**, *33*, 359.
[14] J. R. Ropchan, J.R. Barrio, *J. Nucl. Med.* **1984**, *25*, 887.
[15] T. Hara, M. Iio, R. Izuchi, T. Tsaukiyama, F. Yokoi, *Eur. J. Nucl. Med.* **1985**, *11*, 275–278.
[16] J. Beliczey, U. Kragl, A. Liese, C. Wandrey, K. Hamacher, H.H. Coenen, T. Tierling. US Patent US 6,355,453 B1, **2002**.
[17] P. D. Shreve, Y. Anzai, R. L. Wahl, *RadioGraphics* **1999**, *19*, 61.
[18] R. N. Krasikova, O. F. Kuznetsova, O. S. Fedorova, Y. N. Belokon, V. I. Maleev, L. Mu, S. Ametamey, P. A. Schubiger, M. Friebe, M. Berndt, N. Koglin, A. Mueller, K. Graham, L. Lehmann, L. M. Dinkelborg, *J. Med. Chem.* **2011**, *54*, 406.
[19] N. Koglin, A. Mueller, M. Berndt, H. Schmitt-Willich, L. Toschi, A. W. Stephens, V. Gekeler, M. Friebe, L. M. Dinkelborg, *Clin. Cancer Res.* **2011**, *17*, 6000.
[20] S. Baek, C.-M. Choi, S. H. Ahn, J. W. Lee, G. Gong, J. S. Ryu, S. J. Oh, C. Bacher-Stier, L. Fels, N. Koglin, C. Hultsch, C. A. Schatz, L.M. Dinkelborg, E. S. Mittra, S. S. Gambhir, D. H. Moon, *Clin. Cancer Res.* **2012**, *18*, 5427.

[21] S. Baek, A. Mueller, Y. S. Lim, H.C. Lee, Y. L. Lee, G. Gong, J. S. Kim, J. S. Ryu, S. J. Oh, S. J. Lee, C. Bacher-Stier, L. Fels, N. Koglin, C. A. Schatz, L. M. Dinkelborg, D. H. Moon, *J. Nucl. Med.* **2013**, *54*, 1.
[22] R. A. Cairns, I. S. Harris, T. W. Mak, *Nat. Rev. Cancer* **2011**, *11*, 85.
[23] T. Hara, F. Yokoi, M. Iio, *Eur. J. Nucl. Med.* **1986**, *12*, 21.
[24] Y. F. Cheung, C. Walsh, *Biochemistry* **1976**, *15*, 3749.
[25] D. R. Grassetti, M. E. Brokke, J. F. Murray, *J. Med. Chem.* **1966**, *9*, 149.
[26] D. S. Flournoy, P. A. Frey, *Biochemistry* **1989**, *28*, 9594.
[27] L. S. Leung, P.A. Frey, *Biochem. Biophys. Res. Commun.* **1978**, *81*, 274.
[28] Y. Avi-Dor, J. Mager, *Biochem. J.* **1956**, *63*, 613.
[29] Y. Pocker, J. E. Meany, C. Zadorojny, *J. Phys. Chem.* **1971**, *75*, 792.
[30] S. M. Ametamey, M. Honer, P. A. Schubiger, *Chem. Rev.* **2008**, *108*, 1501.
[31] For reviews see: (a) H. Vorbrüggen, *Helv. Chim. Acta* **2011**, *94*, 947; (b) S. Takamatsu, S. Katayama, N. Hirose, E. De Cock, G. Schelkens, M. Demillequan, J. Brepoels, K. Isawa, *Nucleos. Nucleot. Nucleic Acids* **2002**, *21*, 849.
[32] F. C. Kokesh. *J. Org. Chem.* **1976**, *41*, 3593.

